Available online at www.sciencedirect.com
ScienceDirect
Journal of the European Ceramic Society 29 (2009) 2185–2191
www.elsevier.com/locate/jeurceramsoc

Characterisation of fluorine containing glasses and glass-ceramics by ^{19}F magic angle spinning nuclear magnetic resonance spectroscopy

R.G. Hill [a], R.V. Law [b], M.D. O'Donnell [a,b,*], J. Hawes [b], N.L. Bubb [c], D.J. Wood [c], C.A. Miller [d], M. Mirsaneh [e], I. Reaney [e]

[a] *Department of Materials, Imperial College, London SW7 2BP, UK*
[b] *Department of Chemistry, Imperial College, London SW7 2BP, UK*
[c] *Leeds Dental Institute, University of Leeds, Leeds LS2 9LU, UK*
[d] *The School of Clinical Dentistry, The University of Sheffield, Sheffield S10 2TA, UK*
[e] *Department of Engineering Materials, The University of Sheffield, Sheffield S1 3JD, UK*

Received 10 July 2008; received in revised form 18 December 2008; accepted 13 January 2009
Available online 28 February 2009

Abstract

^{19}F magic angle spinning nuclear magnetic resonance (MAS-NMR) spectroscopy was used to characterise the local environment of fluorine in three types of fluorine containing glass-ceramics. The glass-ceramic compositions studied included four that crystallised to fluorcanasite, one which crystallised to barium fluorphlogopite and one which crystallised to fluorrichterite. In the fluorcanasite glasses, prior to crystallisation, the fluorine was present solely as an F–Ca(n) species whilst following crystallisation it was also present as an F–Ca(n) species in the fluorcanasite phase and in those glasses containing $AlPO_4$ it was also present as an F–Ca(n) species in fluorapatite.

In the fluorrichterite and fluorphlogopite glasses the fluorine was present predominantly as F–Mg(3) and following crystallisation it was also present as F–Mg(3) in the fluorrichterite and fluorphlogopite phases. In all these glass-ceramics fluorine appears to be preferentially associated with the cations of highest charge to size ratio and the local environment of fluorine in the glass and the crystal phase is almost identical.

Keywords: Glass-ceramic; NMR; Oxyfluoride

1. Introduction

There are a significant number of synthetic glass-ceramics that have been developed based on fluorine containing crystal phases. Examples include fluorapatite ($Ca_5(PO_4)_3F$),[1–3] potassium fluorphlogopite ($K_2Mg_6Si_6Al_2O_{18}F_4$),[4–6] fluorrichterite ($KNaMg_5Si_8O_{22}F_2$)[5,7,8] and fluorcanasite ($(Na,K)_6Ca_5Si_{12}O_{30}F_4$).[9] These phases are the fluorine analogues of the natural hydroxyl containing mineral phases. The fluorine analogues are utilised for two reasons; fluorine has a similar charge to size ratio as a hydroxyl ion and fluorine is easier to retain in the glass melt.

Solid state MAS-NMR is a powerful technique for characterising solids and gives information on co-ordination states, next nearest neighbours, bond lengths and bond angles. Whilst nuclei such as ^{29}Si, ^{27}Al, ^{7}Li and ^{31}P have been widely used to characterise minerals, glasses and glass-ceramics,[10,11] there are very few studies of ^{19}F magic angle spinning nuclear magnetic resonance (MAS-NMR) applied to glasses and glass-ceramics. Development of MAS probes with spinning rates > 20 kHz have contributed to reduction in line broadening and minimising the need for multiple pulse techniques.[12] The ^{19}F nucleus is 100% abundant and is the most sensitive nucleus after hydrogen, with a spin = 1/2 and with a large degree of chemical shift anisotropy. The chemical shift of ^{19}F ranges from +500 ppm to −500 ppm thus the chemical shift of fluorine is very sensitive to its chemical environment. The observed ^{19}F chemical shift has been shown to correlate with the fluorine-cation distance in alkali metal fluorides.[13]

Different aspects affecting the co-ordination of F^- in F-bearing silicates and aluminosilicates have also been examined.[13–17] An investigation into the competition between

* Corresponding author. Current address: Bioceramic Therapeutics Ltd., London, UK.
E-mail address: mdo@bioceramictherapeutics.com (M.D. O'Donnell).

0955-2219/$ – see front matter © 2009 Published by Elsevier Ltd.
doi:10.1016/j.jeurceramsoc.2009.01.009

Table 1
Composition of the glasses studied in mole%.

	Na_2O	K_2O	BaO	CaO	CaF_2	MgO	MgF_2	Al_2O_3	P_2O_5	SiO_2
Can 1	10.00	5.00	0.00	15.00	10.00	0.00	0.00	0.00	0.00	60.00
Can 2	9.76	4.88	0.00	14.63	9.76	0.00	0.00	1.22	1.22	58.54
Can 3	9.52	4.76	0.00	14.29	9.52	0.00	0.00	2.38	2.38	57.14
Can 4	3.80	5.10	0.00	19.20	10.30	0.00	0.00	0.00	0.00	61.60
BFP	0.00	0.00	6.52	2.61	0.00	27.25	13.04	7.68	0.87	42.03
F1	3.33	3.33	0.00	0.00	6.62	33.35	0.00	0.00	0.00	53.37

cations of different field strengths to form F–M(n) species[12] demonstrates that F preferentially bonds to higher field-strength modifier cations. In another study, NMR analysis was performed on alumino-silicate-lanthanum fluoride glasses. As well as LaF_3 species forming there was also evidence of Si–F and Al–F bonding. Zeng and Stebbins[17] have investigated the reduction of bridging oxygens (BOs) and formation of Al–F in aluminosilicates when F^- is added and attempted to establish how this is dependent on the chemical composition of the glass. The proportion of non-bridging oxygens (NBOs) upon addition of F^-, in conjunction with the amount and type of modifying cations and competition between modifying cations, Al and Si for F^- ions, all disrupt the silicate and aluminosilicate network. This in turn affects the macroscopic properties of the glass. It is still not understood which of these factors is dominant in determining how F^- co-ordinates and this aspect requires further investigation.

A major drawback to ^{19}F MAS-NMR is that parts of the NMR instrument, probe and rotor are often constructed from machinable ceramic. For example a fluormica glass-ceramic in the probe or the fluorinated polymer rotor cap. There is thus a considerable ^{19}F background signal. However with care this signal can be eliminated by a number of background techniques. The MAS speed of the rotor can also be a problem, due to overlap of spinning sidebands with the central resonance in the material making quantitative characterisation of species difficult. This is further complicated by dipolar broadening in crystalline materials and exacerbated by the peak broadening seen in amorphous materials. This paper characterises three types of glass-ceramic systems based on; fluorphlogopite (FP), fluorrichterite (FR), and fluorcanasite (FC) using ^{19}F MAS-NMR. Previous studies by Stamboulis et al.[18,19] have investigated calcium fluorapatite (FAP) glass-ceramics and mixed calcium/strontium fluorapatite glass-ceramics.[20]

Table 2
Heat treatments used for the glass-ceramics.

Glass-ceramic	Heating rate ($^\circ C\,min^{-1}$)	Heat treatment
Can 1	10	695 °C 1 h and 780 °C 1 h
Can 2	10	720 °C 1 h and 825 °C 1 h
Can 3	10	750 °C 1 h and 850 °C 1 h
Can 4a	5	650 °C 2 h
Can 4b	5	850 °C 2 h
BFP	10	644 °C 2 h and 1225 °C 5 h
F1a	5	650 °C 4 h
F1b	5	700 °C 4 h
F1c	5	800 °C 4 h
F1d	5	900 °C 4 h

2. Experimental

2.1. Binary fluoride salts

Reagent grade CaF_2, SrF_2, MgF_2 and BaF_2 were obtained and used to construct a reference plot of chemical shift against the fluoride ion–metal cation distance.

2.2. Glass compositions

Glasses were melted with reagent grade SiO_2, Na_2CO_3, K_2CO_3, $CaCO_3$, CaF_2, P_2O_5, Al_2O_3, $BaCO_3$, MgO and MgF_2. The nominal glass compositions are given in Table 1 and further details of processing can be found in the references below. They consist of:

- Four canasite glass-ceramics (Can 1–4), one based on the stoichiometry of fluorcanasite ($Na_4K_2Ca_5Si_{12}O_{30}F_4$), another two with 0.25 and 0.5 M additions of Al_2O_3 and P_2O_5 and finally a calcium oxide rich fluorcanasite.[21–23]
- A fluorphlogopite glass-ceramic (BFP) based on the ternary composition 90% barium fluorphlogopite ($Ba_{0.5}Mg_3Si_3AlO_{10}F_2$), 4% cordierite ($Mg_2Al_4Si_5O_{18}$), 6% tricalcium phosphate ($Ca_3(PO_4)_2$).[24]
- A stoichiometric fluorrichterite ($KNaMg_5Si_8O_{22}F_2$) glass-ceramic composition termed F1.[25]

2.3. Heat treatments

The heat treatments for the glass-ceramics are summarised in Table 2.

2.4. ^{19}F MAS-NMR

The ^{19}F measurements were conducted at a resonance frequency of 188.29 MHz, using an FT-NMR spectrometer (DSX-200, Bruker, Germany). The spinning rate of the sample at the magic angle was 15 kHz which would position the spinning sidebands around ±80 ppm from the central resonance. The recycle time was 120 s for ^{19}F. The ^{19}F spectra were recorded using DEPTH pulse sequence to suppress the probe background.[26] The reference material for the chemical shift (in ppm) was CaF_2 taken as −108 ppm relative to the more common standard of $CFCl_3$.

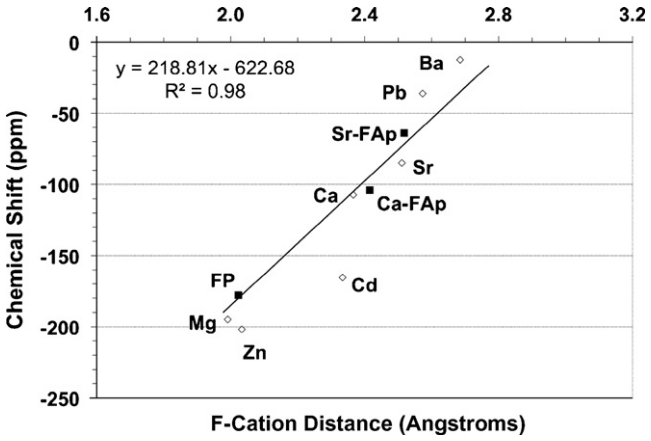

Fig. 1. Chemical shift against F-cation distance open diamonds values taken from the literature. FP = fluorphlogopite and FAP = fluorapatite. ◊ = data from[27]: Zn = ZnF_2, Mg = MgF_2, Cd = CdF_2, Ca = CaF_2, Sr = SrF_2 and Pb = PbF_2 and Ba = BaF_2.

2.5. X-ray powder diffraction

X-ray powder diffraction using Cu K_α radiation was used to characterise the crystal phases formed on heat treatment of the glasses.

3. Results and discussion

Fig. 1 shows the chemical shifts for ^{19}F plotted against the fluorine-cation distance obtained from crystallography data for a range of binary compounds.[27] In a similar fashion to alkali metal fluorides there is a linear relationship between bond distance and the observed chemical shift.[28] Chemical shifts were calculated from the F-cation distances for the crystalline phases found in the glass-ceramics from the literature: fluorcanasite,[29] tetrasilicic fluormica[30,31] and fluorrichterite.[32] The data for the other fluorine containing phases; fluorphlogopite, calcium fluorapatite, strontium fluorapatite from previous studies[18–20,33] are shown on the plot in Fig. 1 and Table 3 and were used to generate the line of best fit in addition to the NMR data on binary fluoride salts.

Table 3
^{19}F chemical shifts of crystalline species.

Phase	δ (ppm)	Refs.
Fluorapatite	−103	[18–20,33]
Fluorite	−108	[27]
Fluorcanasite	−116	This work
NaF	−225	[27]
Si–F	−130	[12]
Al–F–Ca(*n*)	−150	[17]
MgF_2	−170	[27]
Al–F–Mg(*n*)	−150	[35]
Fluorphlogopite	−178	[36]
Fluorrichterite	−174	This work

3.1. Fluorcanasite

Fig. 2 shows the ^{19}F MAS-NMR spectra for the stoichiometric canasite composition. Can 1. The base glass exhibits a single broad peak at about −108 ppm corresponding to F–Ca(*n*). Fluorite has a chemical shift of −108 ppm, but the peak for the glass is much broader than that observed for the fluorite crystal phase, however we can say that the fluorine in the glass is in a fluorite like environment. There is surprisingly no evidence of F–Na(*n*), F–K(*n*) or Si–F species. On heat treatment at 695 °C for 1 h and then 780 °C for 1 h, the peak appears to split slightly suggesting that the presence of CaF_2 (fluorite) at −108 ppm and fluorcanasite at about −116 ppm. The spinning side band to the right at about −225 ppm is slightly shifted and amplified suggesting a trace of an F–Na(*n*) species is present.[27]

The ^{19}F MAS-NMR spectra for the two glass compositions with added Al_2O_3 and P_2O_5 (Can 2 and 3) are shown

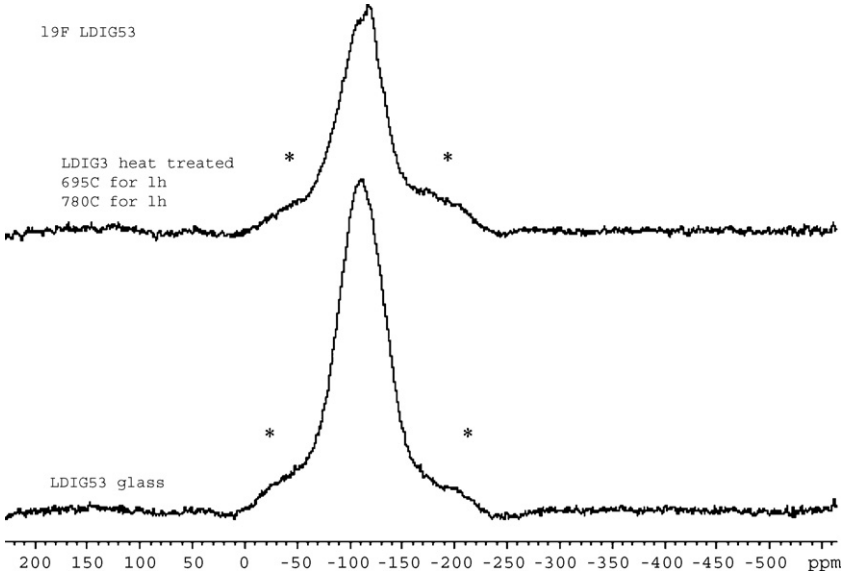

Fig. 2. ^{19}F MAS-NMR traces for a stoichiometric fluorcanasite glass and the glass heat treated for 1 h at 695 and 1 h at 780 °C. * = spinning side band.

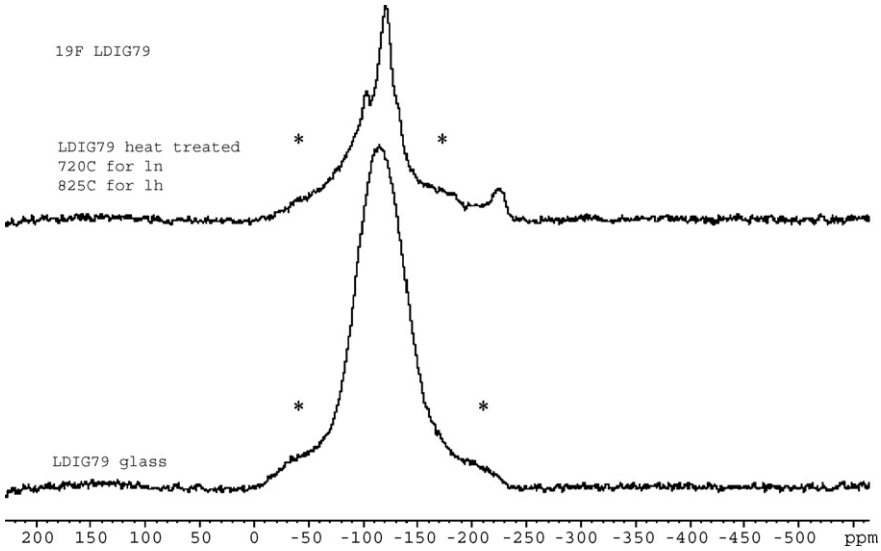

Fig. 3. ^{19}F MAS-NMR traces for a stoichiometric fluorcanasite glass Can 2 with 0.25 mole of Al_2O_3 and P_2O_5 and the same glass heat treated for 1 h at 710 °C and 1 h at 825 °C. * = spinning side band.

in Figs. 3 and 4. Previous studies of calcium and sodium fluoro-alumino-silicates have shown evidence of Al–F–Ca(*n*) and Al–F–Na(*n*) species[12,17] however in these samples there is no evidence of Al–F–Ca(*n*), Al–F–Na(*n*) or Al–F–K(*n*) type species. Essentially all the fluorine is still in a fluorite type environment. On heat treating the Can 2 glass at 720 °C for 1 h and then at 825 °C for 1 h there are three peaks at about −103 ppm, −116 ppm and −225 ppm corresponding to fluorapatite, fluorcanasite and F–Na(*n*).[27] Fluorcanasite was identified on the basis of its predicted chemical shift based on the F-calcium distance obtained from.[29] The canasite is present in much greater amounts than the fluorapatite. There is a broad background suggesting there is appreciable fluorine in the residual glass phase as F–Ca(*n*) type species and there is a weak shoulder at about −150 ppm corresponding to Al–F–Ca(*n*) (Table 3).

On crystallisation of the Can 3 glass at 750 °C for 1 h and then 850 °C for 1 h, the glass shows a peak at −103 ppm corresponding to fluorapatite and a shoulder at about −116 ppm corresponding to fluorcanasite. The peak at −103 ppm is the strongest suggesting there is more fluorapatite in this sample than fluorcanasite and there is more fluorapatite than in the Can 2 sample. The peak is quite broad and there is probably a significant fluorine content in the residual glass with F–Ca(*n*) Al–F–Ca(*n*) and Al–F–Na(*n*) species.

The XRD patterns of these two glasses showed only fluorcanasite following the chosen heat treatment; fluorapatite was not detected. However, a glass with slightly higher Al_2O_3 and P_2O_5 content was found to crystallise to fluorapatite on casting from the melt so the detection of fluorapatite is not unlikely. MAS-NMR is sensitive to short range local order or structure, whilst

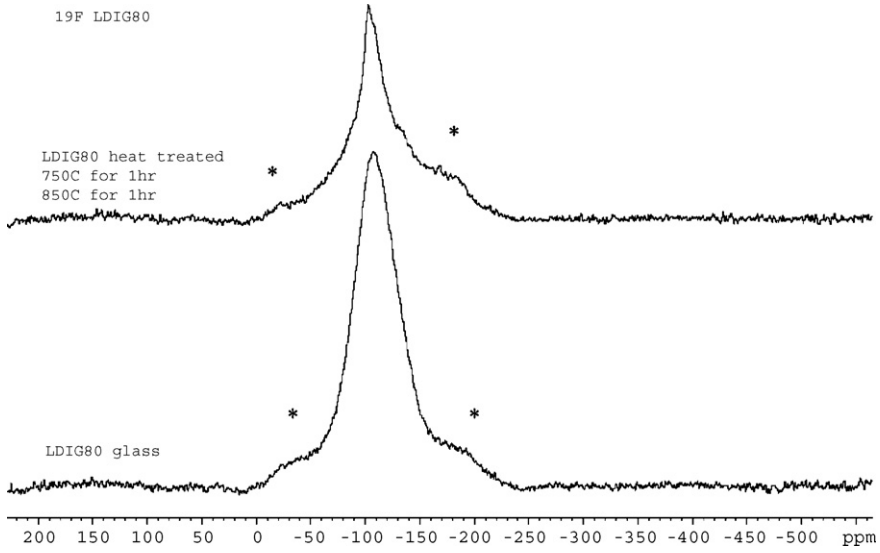

Fig. 4. ^{19}F MAS-NMR traces for a stoichiometric fluorcanasite glass Can 3 with 0.5 mole of Al_2O_3 and P_2O_5 and the same glass heat treated for 1 h at 710 °C and 1 h at 825 °C. * = spinning side band.

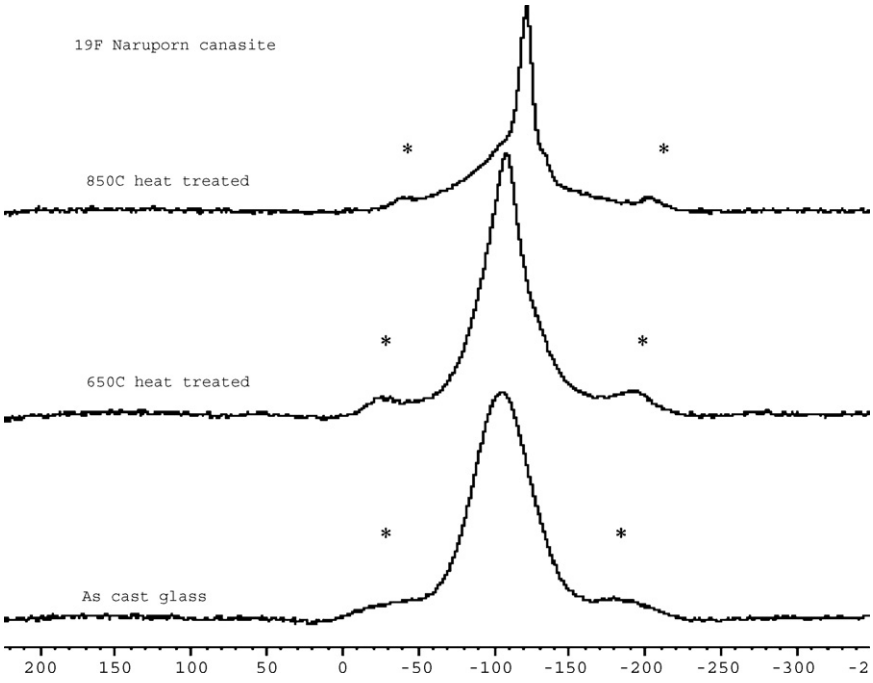

Fig. 5. ^{19}F MAS-NMR spectra for the Can 4 fluorcanasite glass-ceramic. * = spinning side band.

XRD detects long range periodic order. MAS-NMR is capable of detecting the earliest stages of fluorapatite crystallisation since unlike XRD it is not sensitive to crystallite size effects.[20,33]

Can 4 has, like the other canasite glasses a ^{19}F spectra (Fig. 5) that is similar to fluorite with a broad peak at about 108 ppm. On heat treating at 650 °C for 2 h the ^{19}F spectra shows a much sharper peak at 108 ppm corresponding to fluorite. Many fluorcanasite glass-ceramics are widely known to crystallise to fluorite prior to the crystallisation of canasite.[9,23,34] This heat treatment has also been found to result in the crystallisation of fluorite by XRD.[23] On heat treating to 850 °C for 2 h there is a new sharp peak at −116 ppm that we have previously associated with fluorcanasite. There is probably some F–Ca(n) species in the residual glass, plus there is a slight shoulder at about −130 ppm that may correspond to an Si–F species.[12]

3.2. Barium fluorphlogopite (BFP)

The ^{19}F MAS-NMR spectrum for the BFP glass is shown in Fig. 6. This is a glass with the composition 90 mole% barium fluorphlogopite 6 mole% tricalcium phosphate, 4 mole% cordierite. The NMR trace of the base glass shows two peaks at about −100 ppm and about −170 ppm. These are associated with F–Ca(n) and F–Mg(n).[27] There is much more F–Mg(n) than F–Ca(n) as expected on the basis of the composition of this glass. The asymmetric tail to the F–Mg(n) peak could possibly indicate a small amount of Al–F–Mg(n) which would be expected to be seen at approximately −150 ppm.[13,35]

Fig. 6 shows the ^{19}F MAS-NMR spectrum of the heat-treated glass that XRD shows to have crystallised to barium fluorphlogopite (a trisilicic mica). There is a single very sharp line at about −178 ppm corresponding to F–Mg(n) where n is close to 3 that is an exact match to the chemical shift of fluorphlogopite[36] and corresponds to the fluorine in the brucite layer. There is a small peak at about −150 ppm, which is quite sharp that corresponds to a very small amount of a highly ordered phase containing/corresponding to Al–F–Ca(n)[17] or Al–F–Mg(n).[13,35] There is very little fluorine left in the residual glass phase (<10%).

3.3. Fluorrichterite ($KNaCaMg_5Si_8O_{22}F_2$)

Fig. 7 shows the MAS-NMR spectrum of the as cast glass F1 which shows two broad peaks corresponding to F–Ca(n) at about −100 ppm and F–Mg(n) at about −170 ppm.[27] There is more F–Mg(n) than F–Ca(n) and there is much more Mg than Ca in the composition. After heat treating at 650 °C for 4 h a new peak forms at −178 ppm that is identical to the chemical shift observed for fluorphlogopites.[36] This peak corresponds to

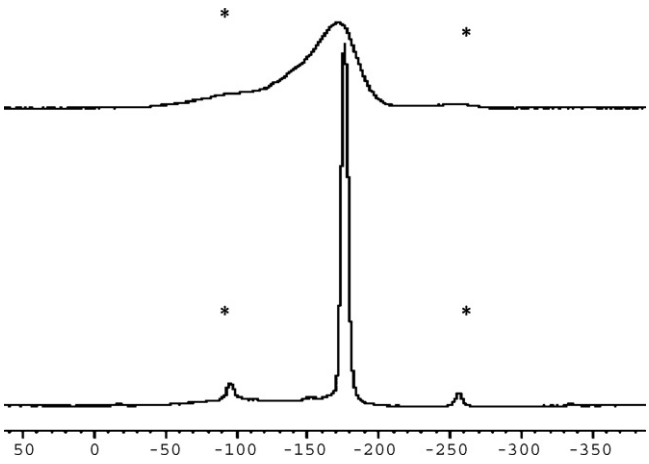

Fig. 6. ^{19}F MAS-NMR spectra for the barium fluorphlogopite glass-ceramic. * = spinning side band.

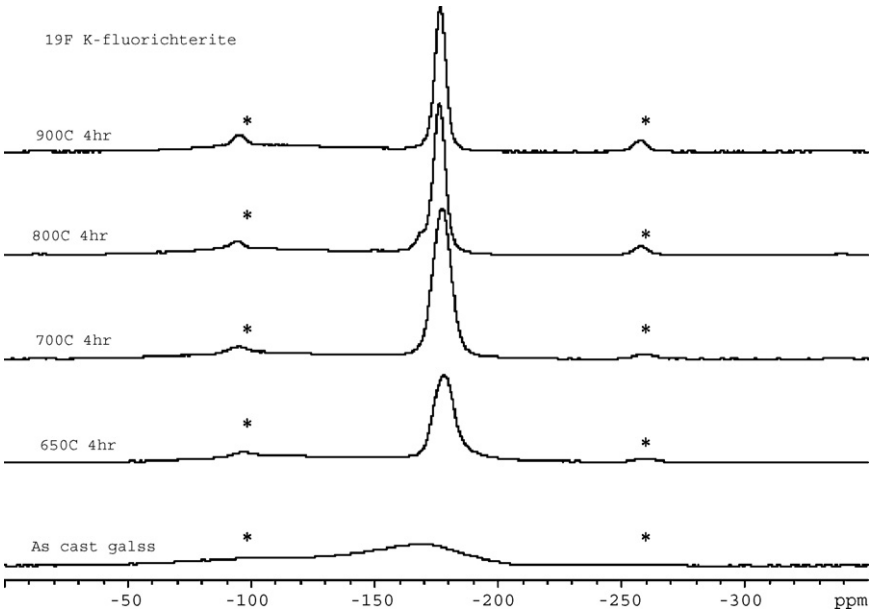

Fig. 7. ^{19}F MAS-NMR spectra for the F1 fluorrichterite glass-ceramic. * = spinning side band.

F–Mg(n) in the brucite layer. Our interpretation of this data is that this peak corresponds to the fluorine in the tetrasilicic mica plus possibly some fluorine in an F–Mg(n) type environment in the residual glass, since it is not quite as sharp as might be expected. On heat treating at 700 °C for 4 h the same peak is present, but is now somewhat sharper suggesting possibly further crystallisation of the tetrasilic mica, plus loss of the F–Mg(n) species in the residual glass. On heat treating to 800 °C for 4 h, a new peak develops that is sharper than the peak at 700 °C and has a slightly reduced chemical shift (about −174 ppm). This heat treatment corresponds to the formation of two crystalline phases determined by XRD (Fig. 8), a tetrasilicic mica and a fluorrichterite phase. It might be expected that a broader peak would occur if we do not resolve the ^{19}F signal from these two phases. However, since there is relatively little of the tetrasilicic mica phase and the major peak corresponds to the fluorrichterite phase, this is not the case. We can establish whether the fluorrichterite phase would have a chemical shift of about −174 ppm by plotting the chemical shift against the F–Mg distance, since there is a strong correlation between chemical shift and F-cation distance. The F–Mg distance in fluorrichterite is 2.014 Å[32] and this correlates well with the observed chemical shift (Fig. 1). There is a small shoulder at about −165 ppm, which remains unassigned. At 900 °C we have a single peak at about −175 ppm which probably corresponds to the fluorrichterite phase. There is surprisingly little fluorine left in the residual glass phase.

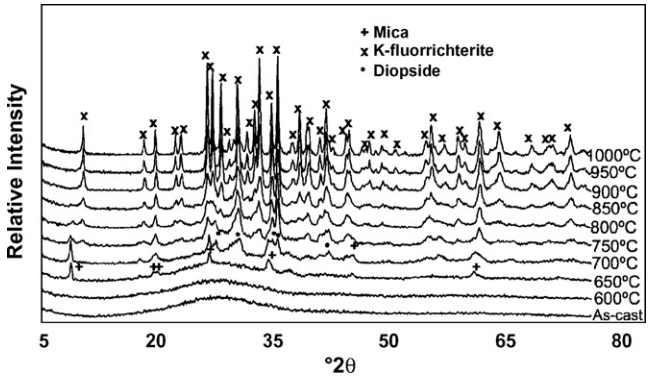

Fig. 8. XRD traces of stoichiometric K-fluorrichterite heat-treated at different temperatures[25].

4. Conclusions

One of the most interesting aspects of this study is that the co-ordination environment of the fluorine in the glass appears to be similar or in many cases almost identical to the first phase that crystallises from the glass and where subsequent crystals form the co-ordination environment of the fluorine is often retained in the final crystal structure. Thus in the fluorphlogopite and fluorrichterite glass-ceramics the F–Mg(3) species is present in the glass and in the crystal structure. The fluorphlogopite glass-ceramic composition studied did not crystallise to precursor crystal phases, but directly to barium fluorphlogopite. In contrast to this, the commercial material Macor™ is known to undergo a complicated crystallisation sequence involving glass in glass, or amorphous phase separation to a magnesium rich matrix phase and aluminium–silicon rich droplet phase. This is then followed by crystallisation of chondrodite $2Mg_2SiO_4{\cdot}MgF_2$, which crystallises in the magnesium rich matrix at the interface of the aluminium and silicon rich droplet phase. The chondrodite phase then transforms to norbergite $MgSiO_4{\cdot}MgF_2$, which finally reacts with components in the residual glass phase to form fluorphlogopite and a minor amount of mullite. Both the two precursor phase have the brucite layer structure, that is also found in the fluorphlogopite crystal and thus the F–Mg(3) species is probably retained from the glass to the final crystal structure.[27] Similarly, in the fluorcanasite glass-ceramics there are present in the glass F–Ca(n) species that have

a chemical shift close to that of fluorite and the same species are present in both the precursor crystal phase and the final crystal phase. A similar situation also exists in the fluorapatite glass-ceramics where we have F–Ca(n) species in the glass and in the fluorapatite crystal phase.[20] Thus the authors propose that the local environment of fluorine in the glass reflects the fluorine structure of the crystal phase or phases that form on heat treatment.

References

1. Hill, R. G. and Wood, D., Apatite mullite glass-ceramics. *Journal of Materials Science: Materials in Medicine*, 1995, **6**(6), 311–318.
2. Kokubo, T., Ito, S., Sakka, S. and Yamamuro, T., Formation of a high-strength bioactive glass ceramic in the system MgO–CaO–SiO_2–P_2O_5. *Journal of Materials Science*, 1986, **21**(2), 536–540.
3. Rafferty, A., Clifford, A., Hill, R. G., Wood, D., Samuneva, B. and Dimitrova-Lukacs, M., Influence of fluorine content in apatite–mullite glass-ceramics. *Journal of the American Ceramic Society*, 2000, **83**(11), 2833–2838.
4. Chyung, K., Beall, G.H. and Grossman, D.G., Fluorphlogopite mica glass-ceramics. Tokyo, Japan: International Glass Congress 14, Kyoto, Japan, 1974.
5. Hench, L. L. and Freiman, S. W., In *Advances in nucleation and crystallization in glasses: symposium*. American Ceramic Society, Columbus, OH, 1971.
6. Thomas, G., Fulrath, R. M. and Fisher, R. M., In *Electron Microscopy and Structure of Materials: Proceedings*. University of California Press, Berkeley, 1972.
7. Beall, G.H. and Megles, J.J.E., Potassium fluorrichterite glass ceramics and method. US Patent 4,467,039, 1984.
8. Beall, G., Chain silicate glass-ceramics. *Journal of Non-Crystalline Solids*, 1991, **129**(1–3), 163–173.
9. Likitvanichkul, S. and Lacourse, W., Effect of fluorine content on crystallization of canasite glass-ceramics. *Journal of Materials Science*, 1995, **30**(24), 6151–6155.
10. Lewis, M. H., *Glasses and glass-ceramics*. Chapman and Hall, London, 1989.
11. MacKenzie, K. J. D. and Smith, M. E.,*Multinuclear solid-state NMR of inorganic materials*, *vol. 6*. 1st ed. Pergamon, Oxford, 2002.
12. Stebbins, J. F. and Zeng, Q., Cation ordering at fluoride sites in silicate glasses: a high-resolution F-19 NMR study. *Journal of Non-Crystalline Solids*, 2000, **262**(1–3), 1–5.
13. Kiczenski, T. and Stebbins, J., Fluorine sites in calcium and barium oxyfluorides: F-19NMR on crystalline model compounds and glasses. *Journal of Non-Crystalline Solids*, 2002, **306**(2), 160–168.
14. Huve, L., Delmotte, L., Martin, P., Ledred, R., Baron, J. and Saehr, D., F-19 MAS-NMR study of structural fluorine in some natural and synthetic 2/1 layer silicates. *Clays and Clay Minerals*, 1992, **40**(2), 186–191.
15. Jana, C. and Braun, M., F-19 NMR spectroscopy of glass ceramics containing fluorapatites. *Biomaterials*, 1996, **17**(21), 2065–2069.
16. Miller, J., Fluorine-19 magic-angle spinning NMR. *Progress in Nuclear Magnetic Resonance Spectroscopy*, 1996, **28**, 255–281.
17. Zeng, Q. and Stebbins, J., Fluoride sites in aluminosilicate glasses: high-resolution F-19 NMR results. *American Mineralogist*, 2000, **85**(5–6), 863–867.
18. Stamboulis, A., Hill, R. G., Law, R. V. and Matsuya, S., MAS NMR study of the crystallisation process of apatite–mullite glass ceramics. *Physics and Chemistry of Glasses*, 2004, **45**(2), 127–133.
19. Stamboulis, A., Hill, R. G., Law, R. V. and Matsuya, S., A MAS NMR study of the crystallisation process of apatite–mullite glass-ceramics. *Bioceramics 16*, 2004, **254**(2), 99–102.
20. Hill, R. G., Calver, A., Skinner, S., Stamboulis, A. and Law, R. V., A MAS-NMR and combined Rietveldt study of mixed calcium/strontium fluorapatite glass-ceramics. *Bioceramics 18*, 2006, **309–311**(Pts 1 and 2), 305–308.
21. Bubb, N., Wood, D. and Streit, P., Reduction of the solubility of fluorcanasite based glass ceramics by additions of SiO_2 and $AlPO_4$. *Glass Technology*, 2004, **45**(2), 91–93.
22. Miller, C. A., Kokubo, T., Reaney, I. M., Hatton, P. V. and James, P. F., Formation of apatite layers on modified canasite glass-ceramics in simulated body fluid. *Journal of Biomedical Material Research*, 2002, **59**(3), 473–480.
23. Miller, C., Reaney, I., Hatton, P. and James, P., Crystallization of canasite/frankamenite-based glass-ceramics. *Chemistry of Materials*, 2004, **16**(26), 5736–5743.
24. Bentley, P. M., Kilcoyne, S. H., Bubb, N. L., Ritter, C., Dewhurst, C. D. and Wood, D. J., Kinetic neutron diffraction and SANS studies of phase formation in bioactive machinable glass ceramics. *Biomedical Materials*, 2007, **2**(2), 151–157.
25. Mirsaneh, M., Reaney, I. M., Hatton, P. V. and James, P. F., Characterisation of high fracture toughness K-fluorrichterite-fluorapatite glass ceramics. *Journal of the American Ceramic Society*, 2004, **87**(2), 240–246.
26. Cory, D. and Ritchey, W., Suppression of signals from the probe in bloch decay spectra. *Journal of Magnetic Resonance*, 1988, **80**(1), 128–132.
27. Bureau, B., Silly, G., Buzare, J. and Emery, J., Superposition model for F-19 isotropic chemical shift in ionic fluorides: from basic metal fluorides to transition metal fluoride glasses. *Chemical Physics*, 1999, **249**(1), 89–104.
28. Boden, N., Kahol, P. K., Mee, A., Mortimer, M. and Peterson, G. N., A simple spin–echo experiment for accurate measurement of chemical shifts in solids: application to 19F in metal difluorides. *Journal of Magnetic Resonance*, 1983, **54**(3), 419–426.
29. Rastsvetaeva, R. K., Khomyakov, A. P., Rozenberg, K. A. and Rozhdestvenskaya, I. V., Crystal structure of F-canasite. *Doklady Chemistry*, 2003, **391**, 177–180.
30. McCauley, J. W., Newnham, R. E. and Gibbs, G. V., Crystal structure analysis of synthetic fluorophlogopite. *American Mineralogist*, 1973, **58**, 249–254.
31. Toraya, H., Iwai, S., Marumo, F. and Hirao, M., The crystal structure of taeniolite, $KLiMg_2Si_4O_{10}F_2$. *Zeitschrift fur Kristallographie*, 1977, **146**, 73–83.
32. Cameron, M., Sueno, S., Papike, J. J. and Prewitt, C. T., High temperature crystal chemistry of K and Na fluor-richterites. *American Mineralogist*, 1983, **68**, 924–943.
33. Hill, R. G., Stamboulis, A., Law, R. V., Clifford, A., Towler, M. and Crowley, C., The influence of strontium substitution in fluorapatite glasses and glass-ceramics. *Journal of Non-Crystalline Solids*, 2004, **336**(3), 223–229.
34. Beall, G., Alkali metal, calcium fluorosilicate glass-ceramic articles. US Patent 4,386,162, 1983.
35. Kiczenski, T. J. and Stebbins, J. F., Fluorine-19 NMR study of the environment of fluorine in silicate and aluminosilicate oxyfluoride glasses. In *American Geophysical Union Fall Meeting*, 2002. p. V72B–1319.
36. Fechtelkord, M., Behrens, H., Holtz, F., Fyfe, C., Great, L. and Raudsepp, M., Influence of F content on the composition of Al-rich synthetic phlogopite. Part 1. New information on structure and phase-formation from Si-29, H-1, and F-19 MAS NMR spectroscopies. *American Mineralogist*, 2003, **88**(1), 47–53.